



**Argonne National Laboratory, with facilities in the states of Illinois and Idaho, is owned by the United States government, and operated by The University of Chicago under the provisions of a contract with the Department of Energy.**

**DISCLAIMER**

This report was prepared as an account of work sponsored by an agency of the United States Government. Neither the United States Government nor any agency thereof, nor any of their employees, makes any warranty, express or implied, or assumes any legal liability or responsibility for the accuracy, completeness, or usefulness of any information, apparatus, product, or process disclosed, or represents that its use would not infringe privately owned rights. Reference herein to any specific commercial product, process, or service by trade name, trademark, manufacturer, or otherwise, does not necessarily constitute or imply its endorsement, recommendation, or favoring by the United States Government or any agency thereof. The views and opinions of authors expressed herein do not necessarily state or reflect those of the United States Government or any agency thereof.

## DISCLAIMER

This report was prepared as an account of work sponsored by an agency of the United States Government. Neither the United States Government nor any agency thereof, nor any of their employees, makes any warranty, express or implied, or assumes any legal liability or responsibility for the accuracy, completeness, or usefulness of any information, apparatus, product, or process disclosed, or represents that its use would not infringe privately owned rights. Reference herein to any specific commercial product, process, or service by trade name, trademark, manufacturer, or otherwise does not necessarily constitute or imply its endorsement, recommendation, or favoring by the United States Government or any agency thereof. The views and opinions of authors expressed herein do not necessarily state or reflect those of the United States Government or any agency thereof.

ARGONNE NATIONAL LABORATORY  
9700 South Cass Avenue  
Argonne, Illinois 60439

Erratum for

ANL-NT-40

PACER - A FAST RUNNING COMPUTER CODE  
FOR THE CALCULATION OF SHORT-TERM CONTAINMENT/CONFINEMENT  
LOADS FOLLOWING COOLANT BOUNDARY FAILURE

VOLUME 1: CODE MODELS AND CORRELATIONS

by J. J. Sienicki

**MASTER**

Please substitute the attached report for the similar report previously issued. Cover was incorrectly labeled. Previous report should be destroyed.

June 1997

ANL-NT-40

PACER - A FAST RUNNING COMPUTER CODE FOR THE  
CALCULATION OF SHORT-TERM CONTAINMENT/CONFINEMENT LOADS  
FOLLOWING COOLANT BOUNDARY FAILURE

VOLUME 1: CODE MODELS AND CORRELATIONS

by

J. J. Sienicki

Reactor Engineering Division  
Argonne National Laboratory  
9700 South Cass Avenue  
Argonne, IL 60439

**MASTER**

NT TECHNICAL MEMORANDUM NO. 40

Results reported in the NT-TM series of memoranda frequently are preliminary and subject to revision. Consequently, they should not be quoted or referenced without the author's permission.

**DISTRIBUTION OF THIS DOCUMENT IS UNLIMITED** <sup>HH</sup>

**DTIC QUALITY INSPECTED 4**



## TABLE OF CONTENTS

	<u>Page</u>
ABSTRACT . . . . .	v
1.0 SUMMARY . . . . .	1
2.0 MULTICOMPARTMENT MASS AND ENERGY EQUATIONS . . . . .	7
3.0 INTERCOMPARTMENT FLOWRATES . . . . .	12
4.0 SUPPRESSION POOL MODELING . . . . .	14
5.0 STEAM FORMATION FROM FLASHING . . . . .	17
5.1 Blowdown Phase . . . . .	17
5.2 Decay Heat Removal . . . . .	20
6.0 CONDENSATION UPON STRUCTURE . . . . .	21
7.0 CONTAINMENT/CONFINEMENT SPRAYS . . . . .	25
8.0 NUMERICAL SOLUTION METHODOLOGY . . . . .	26
9.0 SUMMARY . . . . .	31
ACKNOWLEDGMENTS . . . . .	32
REFERENCES . . . . .	33

## LIST OF FIGURES

	<u>Page</u>
1. Illustration of VVER-440 Model V230 Confinement . . . . .	2
2. Example of Nodalization for a VVER-440 Model V230 Confinement . . . . .	3
3. PACER Computational Flow During Problem Setup and Calculation of Transient . .	30

PACER - A FAST RUNNING COMPUTER CODE FOR THE  
CALCULATION OF SHORT-TERM CONTAINMENT/CONFINEMENT LOADS  
FOLLOWING COOLANT BOUNDARY FAILURE

VOLUME 1: CODE MODELS AND CORRELATIONS

by

J. J. Sienicki

ABSTRACT

A fast running and simple computer code has been developed to calculate pressure loadings inside light water reactor containments/confinements under loss-of-coolant accident conditions. PACER was originally developed to calculate containment/confinement pressure and temperature time histories for loss-of-coolant accidents in Soviet-designed VVER reactors and is relevant to the activities of the U. S. International Nuclear Safety Center. The code employs a multicompartment representation of the containment volume and is focused upon application to early time containment phenomena during and immediately following blowdown. Flashing from coolant release, condensation heat transfer, intercompartment transport, and engineered safety features are described using best estimate models and correlations often based upon experiment analyses. Two notable capabilities of PACER that differ from most other containment loads codes are the modeling of the rates of steam and water formation accompanying coolant release as well as the correlations for steam condensation upon structure.



## 1.0 SUMMARY

The PACER (Pressurization Accompanying Coolant Escape from Ruptures) computer code has been developed to calculate pressure loadings inside light water reactor containments and confinements under loss-of-coolant accident (LOCA) conditions. PACER was originally developed to specifically calculate containment/confinement pressure and temperature time histories for LOCAs in VVER designs. It was used in the "Department of Energy's Team's Analyses of Soviet Designed VVERs" in 1987.<sup>1-3</sup> More recently, the code has been applied to calculate time dependent pressure loadings during a design basis LOCA in a generic VVER-440 Model V213.<sup>4</sup>

PACER was developed with the objective of being computationally fast running, easy to use, and (where possible) to incorporate best estimate models and correlations rather than conservative bounding assumptions. These objectives have been principally achieved in two ways. First, the containment is described using a multicompartment representation in which the containment volume is partitioned into a number of compartments or cells. For example, Figure 1 provides an illustration of the VVER-440 Model V230 confinement while Figure 2 shows a representation of the confinement and surroundings in terms of nine cells. Inside each cell, uniform conditions of pressure, temperature, and concentration are assumed. An arbitrary number of compartments may be defined and connected in a fairly general manner. This reduces the complexity of the calculation relative to codes such as GOTHIC<sup>5</sup> which attempt to mechanistically calculate detailed multidimensional flow fields and spatial dependencies within an individual compartment. Second, the modeling in PACER is directed only at early time phenomena occurring over a timescale of the order of tens of minutes following break inception. This eliminates the need to perform detailed multicell calculations of the heatup of the structural walls and equipment, eliminating a significant amount of computation. The restriction to short-term behavior also avoids the need to consider such beyond design basis accident phenomena as hydrogen combustion, core-concrete interactions, and direct containment heating which are treated in codes such as CONTAIN 1.1<sup>6</sup> which are broader in scope and accordingly much larger in size.

Given the conditions of coolant immediately upstream of the break location, PACER calculates the steam and liquid water formation rates as the discharging coolant depressurizes down to the compartment pressure. PACER follows a different approach from most other containment

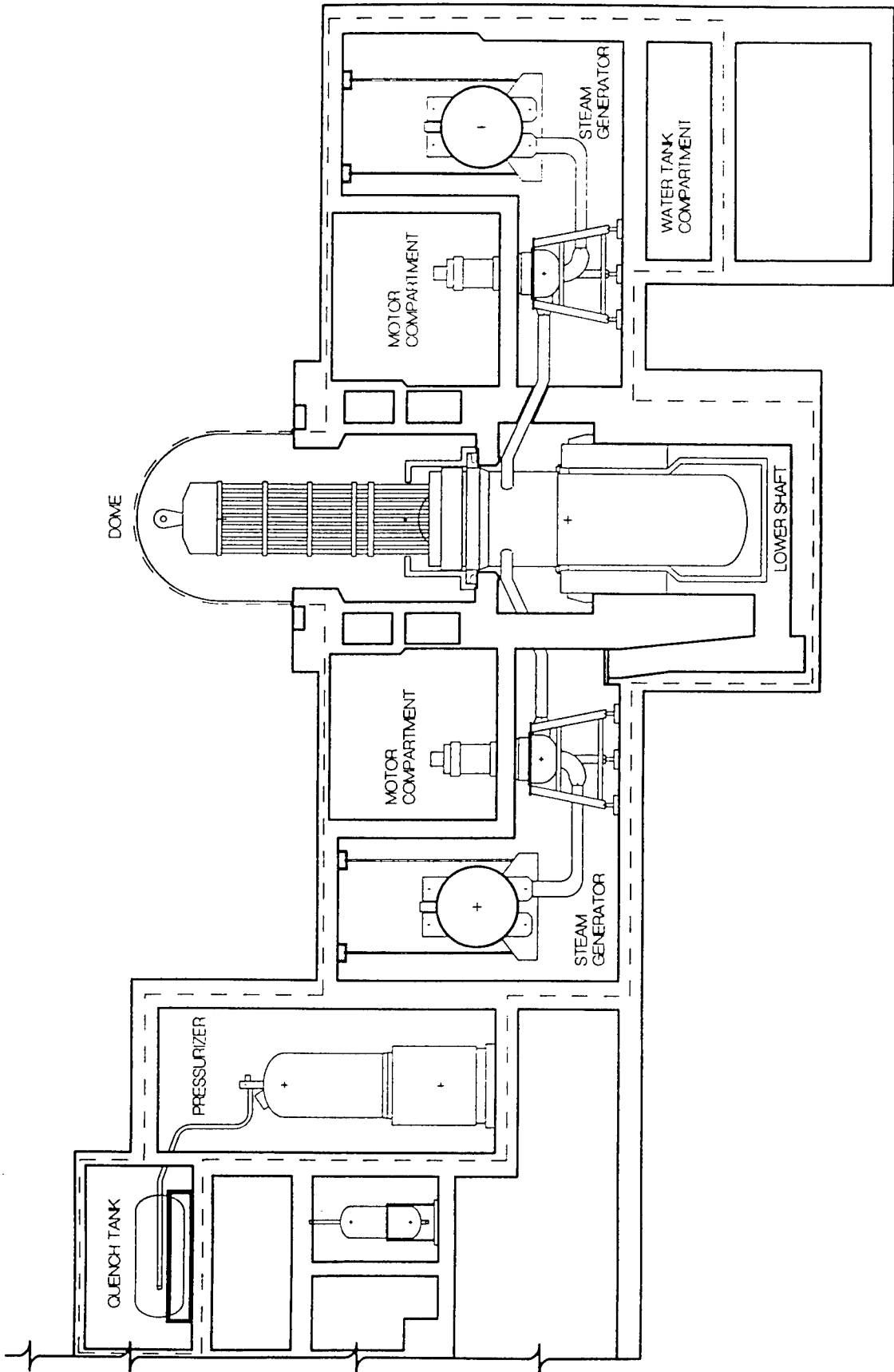


Figure 1. Illustration of VVER-440 Model V230 Confinement

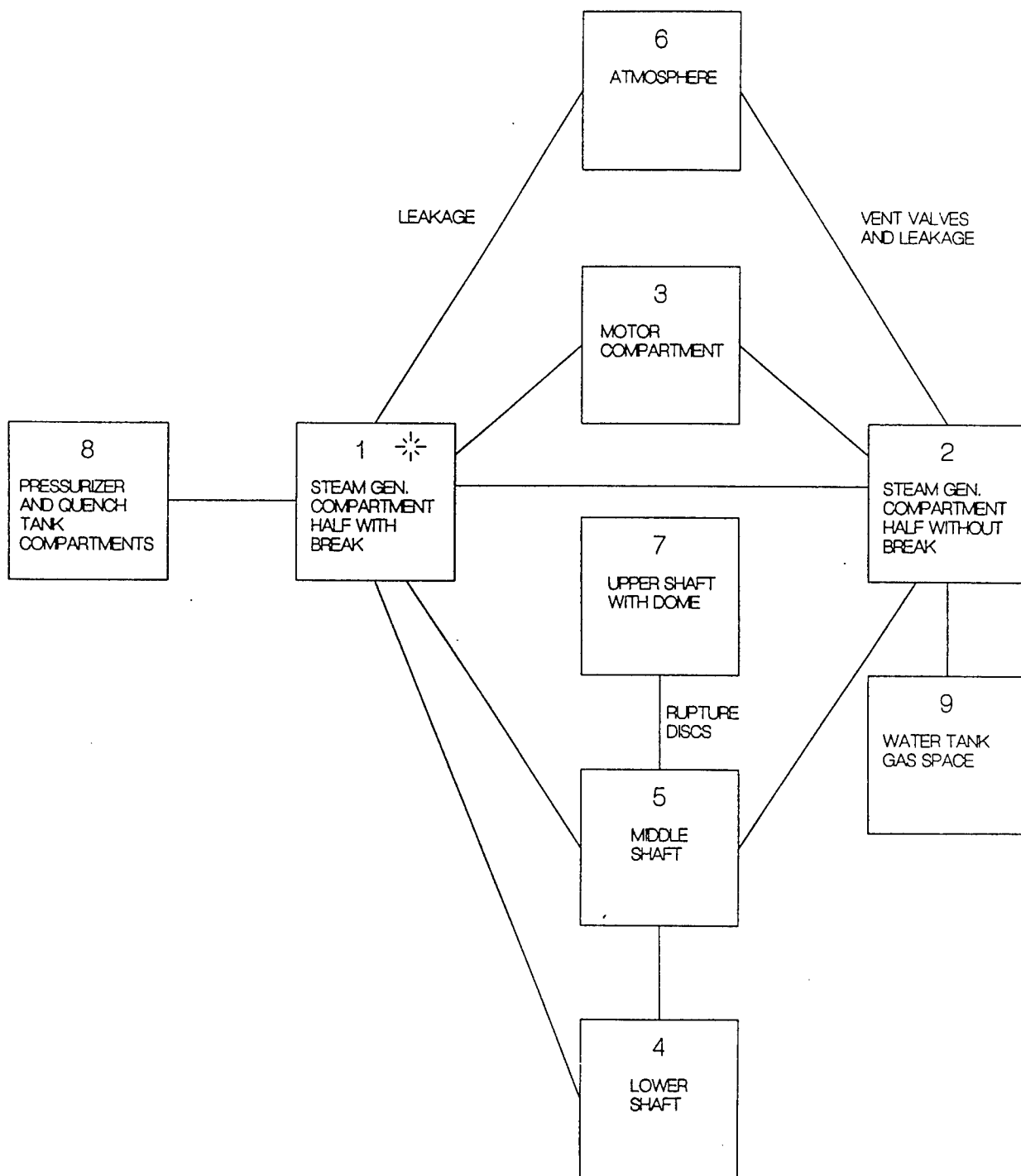


Figure 2. Example of Nodalization for a VVER-440 Model V230 Confinement

loads codes such as CONTAIN 1.1 in calculating steam formation from flashing of released coolant. The PACER approach consists of:

- i) Isentropically expanding coolant released from the break during each timestep down to the cell pressure and determining the separate rates of steam formation and liquid water formation in the vicinity of the break;
- ii) Determining the work performed upon the cell atmosphere during each timestep from isentropic expansion of the released coolant;
- iii) Adding the separate steam and water mass and energy sources formed during each timestep to conservation equations for the steam-gas-water mixture inside the cell atmosphere;
- iv) Adding the work performed on the cell atmosphere as a term in the steam-gas-water mixture energy equation;
- v) Assuming that the steam-gas-water atmosphere remains at saturation at the partial pressure exerted by the steam. Preservation of saturation conditions determines if additional vaporization of the water suspended in the cell atmosphere occurs.

The PACER approach is in contrast to that followed in CONTAIN 1.1 and most other containment loads codes that involves:

- i) Treating the coolant mass and enthalpy released from the break during each timestep as mass and enthalpy sources of superheated liquid water. These sources are added to conservation equations for the steam-gas-water mixture inside the cell atmosphere;

- ii) Assuming that the steam-gas-water mixture remains at saturation at the partial pressure exerted by the steam. Preservation of saturation conditions determines how much steam is formed during each timestep.

The CONTAIN 1.1 assumptions effectively equilibrate the released coolant with the entire steam-gas-water mass inside the cell atmosphere prior to the determination of steam formation. This approach tends to reduce the steam mass that is calculated to be formed. The PACER approach tends to increase the steam mass formed relative to CONTAIN 1.1 because the released coolant flashes prior to equilibration with the steam-gas-water mixture inside the cell atmosphere.

PACER accepts break conditions calculated with a detailed thermal hydraulic code such as RETRAN. This approach is particularly well suited for the use of the RETRAN code, since PACER employs the same functional representations of the steam/water thermodynamic functions as does RETRAN-02.<sup>7</sup> Thus, the steam/water states in the two calculations are consistent. In addition, the code can also determine longer term limiting steam formation rates corresponding to the removal of core decay heat by the emergency core coolant system following primary system depressurization.

PACER solves multicompartment mass equations for steam, air, and entrained water droplets. Water droplets are assumed to be entrained into the steam-air flow, but are envisioned to immediately settle out upon the compartment floor following the completion of the blowdown phase. Steam, air, and (when present) water droplets are assumed to remain in thermal equilibrium at a common compartment atmosphere temperature.

The prediction of intercompartment flows encompasses situations in which pressure differences may exist between neighboring compartments resulting in forced flow. The intercompartment flowrate is determined from the solution of a momentum equation. If entrained water droplets are present, the fraction of droplets carried over from one compartment into another is given by an expression of Schwan<sup>8</sup> based upon experiment analysis. Discharge coefficients for particular flowpaths may be set equal to user-specified values. If desired, strictly one-way flow may be modeled between specific compartments representing the presence of check valves. Natural convection-driven flows are not modeled.

A suppression pool may be defined to exist inside any compartment. Normally, if the water contained in a suppression pool is subcooled, all of the steam entering the pool is assumed to be

condensed. When the pool water is heated to the local saturation temperature, then that fraction of the steam passing through the pool is assumed condensed which maintains the pool in a saturated state. The clearing of water slugs from vertical channels providing access to the pool, which delays the entry of steam into the pool, is modeled in the code.

Condensation upon structure and equipment is calculated using the condensation correlations of Schauer<sup>9</sup> based upon analyses of the HDR, Marviken, and Battelle Frankfurt containment loading experiments. Different correlations describe condensation during the blowdown phase and the period shortly thereafter when forced convection effects are important versus the subsequent post-blowdown period in which natural convection dominates the condensation transport processes and the condensation rate is influenced by the presence of noncondensable gases. The thermal conduction resistance effects of the structure upon condensation are described in terms of simple expressions for the effective time dependent thermal resistance of the concrete walls and steel liners which may be present on the wall inner surfaces. Detailed multicell calculations of the wall heatup are not performed. This approach is adequate for the timescales of tens of minutes or less following break inception over which PACER calculations are carried out given the thick walls and floors typically employed in containment/confinement structures.

Containment/confinement sprays may be defined to exist inside any compartment. It is assumed that a maximum mass of steam is condensed upon the injected water droplets corresponding to removal of the energy represented by the subcooling of the water delivered by the spray system. Cooling of the containment/confinement atmosphere by convective heat transfer to the droplets as well as by convective heat transfer to structural walls is not currently calculated, reflecting the assumption that condensation dominates the short-term atmosphere heat transfer processes.

PACER employs an implicit numerical formulation of the multicompartiment equations and a solution methodology that permits the use of large timesteps thereby reducing the required total number of computational cycles. In practice, the timestep size has been found to be limited only by the accuracy of the first order difference equations.

The modeling and numerical methodology incorporated in PACER makes the code a useful analytical tool for the analysis of containment/confinement loading phenomena under design basis-type accident conditions as well as for beyond design basis ruptures.

## 2.0 MULTICOMPARTMENT MASS AND ENERGY EQUATIONS

The containment/confinement volume is represented in terms of a set of compartments or cells. An arbitrary number of compartments may be defined (as many as twenty-one have been used) and the compartments may be connected in a fairly general manner. The most significant current restriction is that if a suppression pool is defined to exist in the compartment denoted by the index,  $i$ , then the flow into this compartment through the suppression pool must come from the compartment denoted with the index,  $i-1$ .

The containment atmosphere is assumed filled with three constituents. The first is steam generated from the escape and flashing of primary or secondary coolant or present initially as humidity within the atmosphere. The second is a noncondensable gas currently described with properties appropriate for air. The third component, which may or may not be present, corresponds to water droplets which are assumed to be entrained into the atmosphere after exiting the break. If required, additional constituents could be added such as a distinct noncondensable gas field representing hydrogen generated by oxidation.

The time dependent mass of steam inside each compartment satisfies the mass equation,

$$\frac{dM_{v,i}}{dt} = \sum_{j \neq i} A_{j,i} G_{g,j,i} \langle X_v \rangle_{j,i} (1 - F_{pool,v,j,i}) + (GA)_{break,v,i} - S_{cond,v,i} - S_{spray,v,i} + S_{flash,v,i}, \quad (1)$$

where

- $M_{v,i}$  = steam mass inside compartment  $i$ ,
- $t$  = time,
- $A_{j,i}$  = flow area between compartments  $j$  and  $i$ ,
- $G_{g,j,i}$  = mass flux of steam and air between compartments  $j$  and  $i$ ,
- $X_v$  = mass fraction of steam in steam-air mixture,
- $F_{pool,v,j,i}$  = fraction of steam condensed in suppression pool located in compartment  $i$ ,
- $(GA)_{break,v,i}$  = mass formation rate of steam associated with coolant discharging through break,

- $S_{\text{cond},v,i}$  = condensation rate of steam upon structure and equipment in compartment i,  
 $S_{\text{spray},i}$  = condensation rate upon water droplets delivered by sprays in compartment i,  
 $S_{\text{flash},v,i}$  = flashing vaporization rate of steam from water droplets in compartment i,  
v = subscript denoting steam vapor,  
i = subscript denoting i th compartment,  
j = subscript denoting j th compartment,  
g = subscript denoting steam-air mixture.

The mass flux,  $G_{g,j,i}$ , is defined as positive, if the flow is directed from compartment j to compartment i and negative for the case of flow in the reverse direction. It follows that

$$G_{g,i,j} = -G_{g,j,i}. \quad (2)$$

The mass fraction,  $X_v$ , in Equation 1 is that representative of the mixture inside the "upwind" compartment (i.e., the donating compartment). In particular,

$$\langle X_v \rangle_{j,i} = \begin{cases} X_j, & \text{if flow is directed from j to i} \\ X_i, & \text{if flow is directed from i to j} \end{cases} \quad (3)$$

The air mass satisfies a similar conservation equation,

$$\frac{dM_{a,i}}{dt} = \sum_{j \neq i} A_{j,i} G_{g,j,i} \langle X_a \rangle_{j,i}, \quad (4)$$

where

- $M_{a,i}$  = air mass inside compartment i,  
 $X_a$  = mass fraction of air in steam-air mixture.  
a = subscript denoting air.

That portion of the water that remains liquid after the coolant discharging through the break flashes down to the compartment pressure is assumed to be entrained into the atmosphere as water droplets. The droplets are assumed present in the atmosphere only during the blowdown phase when the coolant flowrate from the break is significant. Subsequently, the droplets are envisioned to rapidly settle out to collect as a layer upon the compartment floor. Accordingly, the droplet masses in all compartments are set equal to zero at the end of the blowdown phase which is denoted by a user-specified time. When present, the droplet mass obeys the mass equation,

$$\frac{dM_{d,i}}{dt} = \sum_{j \neq i} A_{j,i} G_{d,j,i} (1 - F_{pool,d,j,i}) + (GA)_{break,d,i} - S_{flash,v,i}, \quad (5)$$

where

- $M_{d,i}$  = water droplet mass inside compartment i,
- $G_{d,j,i}$  = mass flux of water droplets between compartments j and i,
- $F_{pool,d,j,i}$  = fraction of droplets collected at suppression pool located in compartment i,
- $(GA)_{break,d,i}$  = mass formation rate of liquid droplets associated with coolant discharging through break,
- $d$  = subscript denoting water droplets.

The steam, air, and entrained water droplets within each compartment are assumed to remain in thermal equilibrium at a common temperature,  $T_i$ . The formulation of the energy equation depends upon whether or not conditions evolve such that flashing of steam from entrained water droplets occurs. As long as the temperature remains below the saturation temperature at the steam partial pressure or the mass of entrained water is zero, then the temperature satisfies the energy equation,

$$\begin{aligned} & \frac{d}{dt} \left[ (M_{v,i} C_{v,v} + M_{a,i} C_{v,a} + M_{d,i} C_{v,d}) \right] T_i \\ & = \sum_{j \neq i} A_{j,i} G_{g,j,i} \left[ \langle C_{p,v} X_v \rangle_{j,i} (1 - F_{pool,v,j,i}) + \langle C_{p,a} X_a \rangle_{j,i} \right] \langle T \rangle_{j,i} \\ & + \sum_{j \neq i} A_{j,i} G_{d,j,i} (1 - F_{pool,d,j,i}) \langle C_{p,d} T \rangle_{j,i} + (GA)_{break,v,i} C_{v,v} T_{sat,i} \end{aligned}$$

$$\begin{aligned}
& + (GA)_{\text{break,d,i}} C_{v,d} T_{\text{sat,i}} + \left[ (GA)_{\text{break,v,i}} + (GA)_{\text{break,d,i}} \right] w_{\text{sat,i}} \\
& - S_{\text{cond,v,i}} C_{p,v} T_i - S_{\text{spray,v,i}} C_{p,v} T_i,
\end{aligned} \tag{6}$$

where

- $T_i$  = atmosphere temperature inside compartment i,  
 $C_v$  = specific heat at constant volume,  
 $C_p$  = specific heat at constant pressure,  
 $T_{\text{sat,i}}$  = saturation temperature inside compartment i at steam partial pressure inside compartment,  
 $w_{\text{sat,i}}$  = work performed by discharging coolant in expanding from break conditions down to equilibrium state at ambient compartment pressure.

The temperature of the mixture convected into or out of the i th compartment is defined by

$$\langle T \rangle_{j,i} = \begin{cases} T_j, & \text{if flow is directed from j to i and no suppression pool is present between j and i,} \\ T_i, & \text{if flow is directed from i to j and no suppression pool is present between i and j,} \\ T_{\text{pool,i}}, & \text{if flow passes through a suppression pool located in compartment i,} \\ T_{\text{pool,j}}, & \text{if flow passes through a suppression pool located in compartment j,} \end{cases} \tag{7}$$

where

- $T_{\text{pool,i}}$  = temperature of water in suppression pool located in compartment i.

If the mixture temperature calculated with Equation 6 exceeds the saturation temperature at the steam partial pressure, then an amount of entrained water droplets is assumed to vaporize such that saturation equilibrium conditions are attained. In this case, the energy and mass equations are solved in two steps. The first step consists of neglecting the flashing of steam from water droplets and using Equation 6 to estimate a fictitious new temperature accounting for energy exchange from all other processes. The vaporization rate due to flashing of water droplets is calculated from

$$S_{\text{flash,v,i}} = \frac{1}{h_{lv,i}} \left( M_{v,i} C_{v,v} + M_{a,i} C_{v,a} + M_{d,i} C_{p,d} \right) \frac{d}{dt} (T_i - T_{\text{sat,i}}) \tag{8}$$

where

$h_{lv,i}$  = heat of vaporization at steam partial pressure in compartment i.

In the second step, the mixture temperature is set equal to the saturation temperature at the steam partial pressure while the steam and water droplet masses are adjusted for flashing,

$$\frac{dM_{v,i}^{(2)}}{dt} = S_{\text{flash},v,i}, \quad (9)$$

$$\frac{dM_{d,i}^{(2)}}{dt} = -S_{\text{flash},v,i}, \quad (10)$$

where

(2) = superscript denoting that a second updating of the mass is made to reflect the flashing process.

Although flashing is modeled, the effects of partial steam condensation should water subcooling conditions develop are neglected. This assumption is partly motivated by the argument that water droplets will tend to partially fall out of the compartment atmosphere to collect as a water layer upon the floor. Such a layer would have a much lower surface area and, hence, a reduced potential as a source of condensation. The pressure inside the compartment is given by the equation,

$$P_i = (M_{v,i} R_v + M_{a,i} R_a) \frac{T_i}{V_i}, \quad (11)$$

where

$P_i$  = pressure inside compartment i,  
 $R_v$  = gas constant for steam,  
 $R_a$  = gas constant for air,  
 $V_i$  = free volume of compartment i.

### 3.0 INTERCOMPARTMENT FLOWRATES

The velocity between compartments j and i is given by the solution of the momentum equation,

$$\langle \bar{\rho} \rangle_{j,i} L_{j,i} \frac{dU_{j,i}}{dt} + \frac{\langle \bar{\rho} \rangle_{j,i}}{2C_{D,j,i}^2} |U_{j,i}| U_{j,i} = P_j - P_i, \quad (12)$$

where

$$\begin{aligned} \rho &= \text{density,} \\ \bar{\rho} &= \rho_g (1 + Y_{j,i}), \end{aligned} \quad (13)$$

$$\begin{aligned} \rho_g &= \rho_v + \rho_a, \\ \rho_v &= \text{steam density,} \\ \rho_a &= \text{air density,} \\ U_{j,i} &= \text{velocity between compartments j and i,} \\ L_{j,i} &= \text{inertial length for flow between compartments j and i,} \\ C_{D,j,i} &= \text{discharge coefficient for flow between compartments j and i,} \\ Y_{j,i} &= (\rho_g + \rho_d) K_{j,i}^{1/2}, \\ \rho_d &= \text{droplet density,} \end{aligned} \quad (14)$$

$$K_{j,i} = \frac{\gamma - 1}{\gamma} \frac{(1 - \eta)}{(\eta^{2/\gamma} - \eta^{(\gamma+1)/\gamma}) < \rho_g (\rho_g + \rho_d) >_{j,i}}, \quad (15)$$

$$\eta = \begin{cases} P_i/P_j, & \text{if flow is directed j to i} \\ P_j/P_i, & \text{if flow is directed i to j} \end{cases} \quad (16)$$

$$\gamma = \text{specific heat ratio of steam-air mixture.}$$

The factor,  $Y_{j,i}$ , corresponds to the fraction of entrained droplets actually carried over from one compartment to the next. Specifically, not all droplets pass through the interconnecting flow

area. A portion of the droplets are intercepted by structure and de-entrained from the flow. The factor,  $Y$ , defined by Equations 14 through 16 is that recommended by Schwan<sup>8</sup> based upon the analysis of containment loading experiments. The factor,  $Y$ , has a maximum value of

$$Y_{\max} = \frac{\rho_d}{\rho_g} \quad (17)$$

corresponding to the maximum droplet loading of the compartment atmosphere. If the pressure ratio,  $\eta$ , approaches or exceeds a value of unity, then  $Y_{j,i}$  tends to

$$Y_{j,i} = \left( \frac{\langle \rho_g + \rho_d \rangle_{j,i}}{\langle \rho_g \rangle_{j,i}} \right)^{1/2} \quad (18)$$

In general, the presence of droplets entrained in the flow decreases the velocity between compartments tending to restrict the flow of steam from the break compartment and thereby somewhat increasing the magnitude of the peak pressure.

Given the carryover factor,  $Y$ , the mass flux of the steam-air mixture flowing from compartment  $j$  to compartment  $i$  is equal to

$$G_{g,j,i} = \langle \rho_g \rangle_{j,i} U_{j,i} \quad (19)$$

while the droplet mass flux is

$$G_{d,j,i} = \langle \rho_g \rangle_{j,i} Y_{j,i} U_{j,i} \quad (20)$$

The discharge coefficient,  $C_{D,j,i}$ , is defined by the user. Strictly one-way flow may be defined between specific compartments representing the communication of the compartments through check valves.

#### 4.0 SUPPRESSION POOL MODELING

A suppression pool can condense large amounts of steam and significantly cool noncondensable gases passing through the pool water. In PACER, a suppression pool may be defined to exist in any compartment provided that the pool receives flow from the preceding compartment. In particular, if compartment  $i$  possesses a pool, then the flow must enter the pool from compartment  $i-1$ .

PACER assumes that when a suppression pool is subcooled, then all of the steam entering the pool is condensed and air passing through the pool exits at the pool water temperature. The pool condensation factor,  $F_{\text{pool},v,j,i}$ , in Equations 1 and 6 is therefore set equal to a value of unity as long as the pool remains subcooled. Steam condensation in the pool increases its water mass and raises its temperature. The time dependent pool mass is obtained from the equation,

$$\frac{dM_{\text{pool},i}}{dt} = \sum_{j \neq i} A_{j,i} G_{g,j,i} \langle X_v \rangle_{j,i} F_{\text{pool},v,j,i}, \quad (21)$$

where

$$M_{\text{pool},i} = \text{liquid water mass in suppression pool located in compartment } i.$$

From the thermodynamic first law enthalpy equation,

$$dh = Tds + vdP, \quad (22)$$

the specific enthalpy of the pool water satisfies

$$\begin{aligned} M_{\text{pool},i} \frac{dh_{\text{pool},i}}{dt} = & \sum_j A_{j,i} G_{g,j,i} \left\{ \langle X_v \rangle_{j,i} \left[ h_{lv,\text{pool},i} + C_{p,v} (\langle T \rangle_{j,i} - T_{\text{pool},i}) \right] F_{\text{pool},v,j,i} \right. \\ & \left. + \langle X_a \rangle_{j,i} C_{p,a} (\langle T \rangle_{j,i} - T_{\text{pool},i}) \right\} + M_{\text{pool},i} v_{\text{pool},i} \frac{dP_{\text{pool},\text{sat},i}}{dt} \end{aligned} \quad (23)$$

where

- $h_{\text{pool},i}$  = pool water specific enthalpy along the saturation curve,  
 $h_{\text{lv,pool},i}$  = heat of vaporization along saturation curve at pool water temperature,  
 $T_{\text{pool},i}$  = pool water temperature,  
 $v_{\text{pool},i}$  = specific volume along saturation curve at pool water temperature,  
 $P_{\text{pool,sat},i}$  = saturation vapor pressure at pool water temperature.

When the pool temperature,  $T_{\text{pool},i}$ , is calculated to rise to the saturation temperature,  $T_{\text{sat},i}$ , of the atmosphere inside the  $i$  th compartment, then the pool is assumed to remain in a saturated state. In this case, not all of the steam entering the pool is condensed. Instead, only that portion needed to raise the pool temperature the required amount to maintain saturation conditions undergoes condensation. For a saturated pool, the steam condensation factor,  $F_{\text{pool,v},j,i}$ , is therefore generally less than unity. The condensation factor is obtained from the pool enthalpy equation,

$$\begin{aligned}
 M_{\text{pool},i} \frac{dh_{\text{pool},i}}{dt} = & \sum_{j \neq i} A_{j,i} G_{g,j,i} \left\{ \langle X_v \rangle_{j,i} \left[ h_{\text{lv,pool},i} + C_{p,v} (\langle T \rangle_{j,i} - T_{\text{pool},i}) \right] F_{\text{pool,v},j,i} \right. \\
 & \left. + \langle X_a \rangle_{j,i} C_{p,a} (\langle T \rangle_{j,i} - T_{\text{pool},i}) \right\} + M_{\text{pool},i} v_{\text{pool},i} \frac{dP_i}{dt}.
 \end{aligned} \tag{24}$$

In this case,  $h_{\text{pool},i}$ ,  $h_{\text{lv,pool},i}$ , and  $T_{\text{pool},i}$  are the liquid specific internal enthalpy, heat of vaporization, and temperature along the water saturation curve at the ambient compartment pressure,  $P_i$ . Equation 24 can therefore be solved for the condensation factor, if the compartment pressure is known.

It is assumed that entrained water droplets do not enter a suppression pool, but are collected and de-entrained by structure upstream of the entrance to the pool.

Strictly speaking, the inception of steam flow through a suppression pool does not coincide with the onset of a pressure differential between the upstream and downstream compartments. Access to the pool usually requires the displacement of a column of water downward through a vertical channel. Only when the channel has been cleared of the liquid water column can steam and air commence to rise upward through the pool water. In PACER, the timing of the inception of steam condensation in the pool is predicted by modeling the downward expulsion of a liquid slug

through a vertical channel. Specifically, flow through the pool begins when the slug displacement satisfies

$$Z_{\text{slug}} \geq L_{\text{slug}} \quad (25)$$

where

$Z_{\text{slug}}$  = downward displacement of liquid slug,

$L_{\text{slug}}$  = initial water depth inside channel.

The displacement is given by

$$Z_{\text{slug}} = \int_0^t U_{\text{slug}} dt \quad (26)$$

where the velocity,  $U_{\text{slug}}$ , satisfies

$$\frac{dU_{\text{slug}}}{dt} = \frac{P_{i-1} - P_i - \rho_{\text{slug}} Z_{\text{slug}}}{\rho_{\text{slug}} (L_{\text{slug}} - Z_{\text{slug}})} \quad (27)$$

where

$\rho_{\text{slug}}$  = slug water density.

Until the slug has been cleared, the interconnecting area,  $A_{j,i}$ , leading to the suppression pool is equal to zero.

## 5.0 STEAM FORMATION FROM FLASHING

### 5.1 Blowdown Phase

When a break occurs in the primary or secondary system boundary, the coolant exiting the break is initially highly superheated relative to the ambient compartment pressure. The coolant thus undergoes flashing to lower its temperature by converting a portion of the liquid to vapor. Given the conditions of the coolant immediately upstream of the break, the fraction of the coolant mass introduced into the break compartment as steam is calculated in PACER using equilibrium thermodynamics. From the first law enthalpy equation, Equation 22, the enthalpy change in an isentropic expansion is given by

$$dh = vdP. \quad (28)$$

For a two-phase fluid, this provides

$$\frac{d}{dP} \left( h_l + xh_{lv} + \frac{u^2}{2} \right) = v_l + xv_{lv} \quad (29)$$

where

P	=	pressure,
$h_l$	=	liquid specific internal enthalpy along saturation curve at pressure P,
x	=	quality,
$h_{lv}$	=	heat of vaporization along saturation curve,
u	=	fluid velocity,
$v_l$	=	liquid specific volume along saturation curve,
$v_{lv}$	=	$v_v - v_l$ ,
	=	difference between vapor and liquid specific volumes along saturation curve,
$v_v$	=	vapor specific volume along saturation curve.

Since  $h_l$ ,  $h_{lv}$ ,  $v_l$ , and  $v_{lv}$  are all functions of P, Equation 29 can be solved for the final quality. The initial state is taken equal to that where the liquid specific internal enthalpy equals that of the liquid

immediately upstream of the break. In obtaining the quality of the final state corresponding to the compartment pressure, the velocity,  $u$ , is set equal to zero.

In solving Equation 29, it has been found convenient to discretize the pressure interval in terms of equal increments of the logarithm of the pressure whereby

$$\delta \ln P = \frac{\ln P_{\text{final}} - \ln P_{\text{initial}}}{N} \quad (30)$$

where

- $\ln$  = denotes natural logarithm,
- $N$  = number of intervals.

This reflects the logarithmic dependence of the specific enthalpy and liquid specific volume upon the pressure. A value of  $N$  equal to fifty is set internally in the code.

If  $(GA)_{\text{break}}$  is the total mass flowrate through one side of the break, then the steam formation rate is defined as

$$(GA)_{\text{break},v} = (GA)_{\text{break}} x_{\text{final}} \quad (31)$$

where

- $x_{\text{final}}$  = final quality at compartment pressure,

and the liquid discharge rate is

$$(GA)_{\text{break},d} = (GA)_{\text{break}} (1 - x_{\text{final}}). \quad (32)$$

In expanding to the ambient pressure, the flashing coolant performs work upon the surrounding compartment atmosphere and possibly upon structures within the containment. For example, following a large rupture of a primary coolant pipe, a portion of the work potential may be realized in the recoil of the pipe and the energy absorbed by deformable pipe whip restraints. Currently, the work potential is assumed to be performed completely again the

compartment/confinement atmosphere and is therefore added to the energy equation, Equation 6, as an energy source. The work per unit mass of discharged fluid is evaluated from the thermodynamic expression,

$$du = d(h - Pv) = Tds - dw, \quad (33)$$

whereby the work performed in an isentropic expansion is given by

$$w = [h_1 + xh_{lv} - P(v_1 + xv_{lv})]_{\text{initial}} - [h_1 + xh_{lv} - P(v_1 + xv_{lv})]_{\text{final}} \quad (34)$$

where

- w = specific work performed in going from initial state to final state,
- initial = subscript denoting initial state corresponding to conditions immediately upstream of break,
- final = subscript denoting final state at ambient compartment pressure.

In PACER, the break may be specified by the user to be either single- or double-sided. For the case of a double-sided break, separate calculations of the quality and contribution to the work are performed for the coolant flowing from each side.

The determination of the conditions of the coolant immediately upstream of the break location is dependent upon the particular application. The usual approach is to use a detailed, two-phase, thermal hydraulic code such as RELAP5 or RETRAN to calculate the coolant state on each of the two sides of the break. Specific variables required by PACER are the break mass flowrate and the coolant specific internal enthalpy inside the coolant boundary at the break location. The specific internal enthalpy is used to define the pressure of a corresponding saturation state from which the flashing down to the compartment pressure may be evaluated using the method discussed in the preceding section. This approach is particularly well suited for the use of the RETRAN-02 code<sup>7</sup> or more recent versions of RETRAN since PACER employs the same functional representations of the water thermodynamic functions as does RETRAN-02. Thus, the water states in the two calculations are consistent.

## 5.2 Decay Heat Removal

Following depressurization of the primary system, the steam formation rate ultimately reflects the removal of the decay heat from the core provided that the emergency core cooling system (ECCS) remains available and core degradation is averted. In particular, water is delivered into the vessel by the low pressure coolant injection pumps of the ECCS. If the ECCS water is heated to the saturation temperature, then steam formation will take place. When break flow conditions from a system thermal hydraulic code are no longer available, the steam formation rate in this limiting situation is set equal to

$$(GA)_{\text{decay,v}} = \frac{(GA)_{\text{LPI}}}{h_{\text{lv,i,sat}}} \left[ \frac{Q_{\text{decay}}}{(GA)_{\text{LPI}}} - (h_{\text{l,i,sat}} - h_{\text{LPI}}) \right] \quad (35)$$

where

- $(GA)_{\text{LPI}}$  = flowrate of water injection into vessel,
- $Q_{\text{decay}}$  = total core decay heat,
- $h_{\text{lv,i,sat}}$  = heat of vaporization along saturation curve at compartment pressure,
- $h_{\text{l,i,sat}}$  = liquid specific enthalpy along saturation curve at compartment pressure,
- $h_{\text{LPI}}$  = specific internal enthalpy of injected water.

The flowrate in Equation 35 represents water that is actually delivered to the vessel and does not include injected ECCS water that directly flows out of the break without removing energy from the core. It is noted that in the present case, Equation 35 provides the flowrate of steam exiting the break location.

## 6.0 CONDENSATION UPON STRUCTURE

The condensation rate upon structure is related to an overall condensation coefficient by

$$S_{\text{cond},v,i} = \frac{A_{\text{cond},i} H_{\text{cond},i} (T_i - T_{\text{wall}})}{h_{\text{lv},i,\text{sat}}} \quad (36)$$

where

$A_{\text{cond},i}$  = surface area for condensation inside compartment  $i$ ,

$H_{\text{cond},i}$  = condensation coefficient for compartment  $i$ ,

$T_{\text{wall}}$  = initial structural wall temperature.

The overall condensation coefficient is defined in terms of a coefficient,  $H_{v,i}$ , describing the condensation mass transfer in the steam-air phase and a conductance,  $H_{\text{wall}}$ , accounting for the thermal resistance of the structure. In particular,

$$H_{\text{cond},i}^{-1} = H_{v,i}^{-1} + H_{\text{wall}}^{-1} \quad (37)$$

The vapor side coefficient,  $H_{v,i}$ , is assumed equal to that recommended by Schauer<sup>9</sup> based upon analyses of the HDR, Marviken, and Battelle Frankfurt containment loading experiments. Different correlations describe condensation during the blowdown phase and shortly thereafter when turbulent forced convection effects are significant versus the subsequent post-blowdown period in which natural convection dominates the condensation transport processes as well as an intermediate transition period. During the blowdown phase, the coefficient,  $H_{v,i}$ , is given in meter-Kilogram-second units by

$$H_{v,\text{forced}} \left[ \text{W}/(\text{m}^2 \cdot \text{K}) \right] = \frac{630 \rho_g}{L_{\text{cond}}^{0.2}} \left( \frac{7045}{Z_{\text{cond}}^{3.6} + 200} \right)^{0.8} \quad (38)$$

where

$$L_{\text{cond}} = \left( \frac{3V_i}{4\pi} \right)^{1/3}, \quad (39)$$

$L_{\text{cond}}$  = film length,  
 $Z_{\text{cond}}$  = distance of structure from break location.

The length,  $L_{\text{cond}}$ , is set equal to the radius of a sphere having a volume equivalent to that of the compartment as recommended by Schauer.<sup>9</sup> In the break compartment, the distance,  $Z_{\text{cond}}$ , is also taken equal to the equivalent spherical radius, consistent with the recommendation in Reference 9.

Equation 38 applies to the blowdown phase when turbulence effects induced by the jet discharge give rise to forced convection mass transfer of steam to the walls. After completion of the blowdown, the turbulence level decreases with time. Accordingly, the forced convection condensation coefficient in the transition period following blowdown decays exponentially with time as

$$H_{v,\text{tran}} \left[ \text{W}/(\text{m}^2 \cdot \text{K}) \right] = \frac{630 \rho_g}{L_{\text{cond}}^{0.2}} \left( \frac{7045}{Z_{\text{cond}}^{3.6} + 200} \right)^{0.8} \exp \left[ -(0.8) (0.054) (t - t_b) \right] \quad (40)$$

where

$t_b$  = time at the completion of the blowdown phase.

Subsequently, the mass transfer is dominated by natural convection and is significantly influenced by the presence of noncondensable gases. In this case, the vapor side condensation coefficient is given by

$$H_{v,\text{nat}} \left[ \text{W}/(\text{m}^2 \cdot \text{K}) \right] = \frac{8100}{1 + 66 \frac{P_a}{P}} \left[ \frac{1}{D_{\text{cond}} (T_i - T_{\text{wall}})} \right]^{0.25} \quad (41)$$

where

$P_a$  = partial pressure of air inside compartment,  
 $D_{\text{cond}}$  =  $(3V_i/4\pi)^{1/3}$ ,  
 = representative dimension.

The length,  $D_{\text{cond}}$ , is also taken equal to the radius of an equivalent spherical volume as recommended by Schauer.<sup>9</sup> Following the completion of the blowdown, the coefficient,  $H_{v,i}$ , is set equal to the maximum value predicted by Equations 40 and 41 to effect a smooth transition between the two correlations.

In evaluating the thermal effects of the wall, it is assumed that the concrete may be covered with a carbon or stainless steel liner. The wall time dependent thermal resistance is taken equal to

$$H_{\text{wall}}^{-1} = \begin{cases} (\pi\alpha_{\text{liner}} t)^{1/2}, & \text{if } t \leq t_{\text{liner}}, \\ \frac{[\delta_{\text{liner}}^2 + \pi\alpha_{\text{conc}}(t - t_{\text{liner}})]^{1/2} - \delta_{\text{liner}}}{k_{\text{conc}}} + \frac{\delta_{\text{liner}}}{k_{\text{liner}}}, & \text{if } t > t_{\text{liner}} \end{cases}, \quad (42)$$

where

$$\begin{aligned} \alpha_{\text{liner}} &= \text{steel liner thermal diffusivity,} \\ k_{\text{liner}} &= \text{steel liner thermal conductivity,} \\ t_{\text{liner}} &= \frac{\delta_{\text{liner}}^2}{\pi\alpha_{\text{liner}}}, \\ \delta_{\text{liner}} &= \text{steel liner thickness,} \\ \alpha_{\text{conc}} &= \text{concrete thermal diffusivity,} \\ k_{\text{conc}} &= \text{concrete thermal conductivity.} \end{aligned} \quad (43)$$

PACER does not incorporate detailed multicell calculations of the heatup of the steel liner, concrete walls and floors, or other structures and equipment. This approach is adequate for times of the order of tens of minutes following break inception over which calculations are carried out given the thick concrete walls and floors typically employed in nuclear containment/confinement structures. Specifically, the approach is valid until transient thermal wave propagation involves the structural wall thickness or half-thickness.

It is currently assumed in PACER that heat transfer to structures takes place solely by condensation. Concurrent direct forced convection or natural convection heat transfer arising from thermal gradients in the atmosphere near structures are not modeled. It is anticipated that this is an

adequate assumption for the early times following coolant boundary rupture when the heat transfer phenomena are expected to be dominated by condensation. In particular, the water condensing upon structure accumulates as liquid films which would have exposed surface temperatures near the compartment saturation temperature.

## 7.0 CONTAINMENT/CONFINEMENT SPRAYS

Containment/confinement sprays may be defined to exist inside any compartment. It is assumed that a maximum mass of steam is condensed upon the droplets corresponding to the energy represented by the subcooling of the water delivered by the spray system. This is actually an assumption about the spray condensation effectiveness reflecting the size of the droplets produced by the spray nozzles and the droplet fall heights characteristic of the containment configuration. Assuming that the spray droplets are heated from the initial temperature to the compartment saturation temperature, the condensation rate is

$$S_{\text{spray,v,i}} = \frac{(GA)_{\text{spray,i}} (h_{\text{l,i,sat}} - h_{\text{spray}})}{h_{\text{lv,i,sat}}} \quad (44)$$

where

- $(GA)_{\text{spray,v,i}}$  = flowrate of sprays injected into compartment i,
- $h_{\text{l,i,sat}}$  = liquid specific enthalpy along saturation curve at steam partial pressure inside compartment,
- $h_{\text{spray}}$  = initial specific enthalpy of spray water,
- $h_{\text{lv,i,sat}}$  = heat of vaporization along saturation curve at steam partial pressure inside compartment.

## 8.0 NUMERICAL SOLUTION METHODOLOGY

The PACER numerical solution methodology was formulated with the objective of avoiding the need to use very small numerical timesteps to achieve stable computation. The use of large numerical timestep sizes reduces the number of computational cycles that must be performed to advance the equations over a specified time interval. The approach therefore sought to incorporate a suitable degree of "implicitness" into the numerical formulation and solution of the model equations. Implicitness involves formulating quantities at the end of the current timestep. The approach further involves linearizing those end of timestep quantities in the equations that significantly depend upon pressure in terms of the incremental changes in the compartment pressures over the current timestep to obtain equations determining the incremental pressure changes. The major key to success is to identify the significant pressure dependencies to ensure that the relevant quantities are formulated at the end of the current timestep and that the pressure dependencies are accounted for. Quantities that do not have a significant dependency can then be formulated "explicitly" at the beginning of the timestep.

The steam and air mass equations are linearized in terms of the incremental changes in the compartment pressures. The steam mass equation, Equation 1, neglecting flashing from water droplets, is written as

$$\begin{aligned} \frac{\delta M_{v,i}}{\delta t} = & \sum_{j \neq i} A_{j,i} \left( G_{g,j,i}^n + \frac{\partial G_{g,j,i}}{\partial P_j} \delta P_j + \frac{\partial G_{g,j,i}}{\partial P_i} \delta P_i \right) \langle X_v^n \rangle_{j,i} \\ & \left( 1 - F_{\text{pool},v,j,i}^n - \delta F_{\text{pool},v,j,i} \right) + (GA)_{\text{break},v,i}^n - S_{\text{cond},v,i}^n - \frac{\partial S_{\text{cond},v,i}}{\partial P_i} \delta P_i \\ & - S_{\text{spray},v,i}^n - \frac{\partial S_{\text{spray},v,i}}{\partial P_i} \delta P_i \end{aligned} \quad (45)$$

where

$\delta M_{v,i}$  = incremental change in steam mass over timestep,

$\delta t$  = timestep size,

$\delta P_j$  = incremental change in pressure in compartment j over timestep,

$\frac{\partial G_{g,j,i}}{\partial P_j}$  = partial derivative of flowrate with respect to pressure in compartment j,

$\delta F_{\text{pool},v,j,i}$  = incremental change in pool condensation factor over timestep,

n = superscript denoting beginning of timestep value.

The air mass equation, Equation 4, is similarly formulated as

$$\frac{\delta M_{a,i}}{\delta t} = \sum_{j \neq i} A_{j,i} \left( G_{g,j,i}^n + \frac{\partial G_{g,j,i}}{\partial P_j} \delta P_j + \frac{\partial G_{g,j,i}}{\partial P_i} \delta P_i \right) \langle X_a^n \rangle_{j,i}. \quad (46)$$

The appropriate suppression pool enthalpy equation is employed to develop an equation for the incremental change in the pool condensation factor of the form,

$$\delta F_{\text{pool},v,j,i} = a_{\text{pool},i} + b_{\text{pool},i} \delta P_i. \quad (47)$$

For the case of a subcooled pool,

$$a_{\text{pool},i} = 0, \quad (48)$$

$$b_{\text{pool},i} = 0.$$

When the pool water is saturated, Equation 24 is differenced as

$$\begin{aligned} M_{\text{pool},i}^n \frac{dh_{\text{pool},i}}{dP_i} \frac{\delta P_i}{\delta t} = \sum_{j \neq i} A_{j,i} \left( G_{g,j,i}^n + \frac{\partial G_{g,j,i}}{\partial P_j} \delta P_j + \frac{\partial G_{g,j,i}}{\partial P_i} \delta P_i \right) \left\{ \langle X_v^n \rangle_{j,i} \right. \\ \left[ h_{lv,\text{pool},i}^n + \frac{dh_{lv,\text{pool},i}}{dP_i} \delta P_i + C_{p,v} \left( \langle T^n \rangle_{j,i} - T_{\text{pool},i}^n - \frac{dT_{\text{pool},i}}{dP_i} \delta P_i \right) \right] \\ \left. \left( F_{\text{pool},v,j,i}^n + \delta F_{\text{pool},v,j,i} \right) + \langle X_{an} \rangle_{j,i} C_{p,a} \left( \langle T^n \rangle_{j,i} - T_{\text{pool},i}^n - \frac{dT_{\text{pool},i}}{dP_i} \delta P_i \right) \right\} \\ + M_{\text{pool},i}^n v_{\text{pool},i}^n \frac{\delta P_i}{\delta t}. \quad (49) \end{aligned}$$

Retaining only first order terms provides the forward elimination coefficients,  $a_{\text{pool},i}$  and  $b_{\text{pool},i}$ . Substitution of Equation 47 into Equation 45 then yields an equation expressing  $\delta M_{v,i}$  solely in terms of increments in the compartment pressures. At this point, the ideal gas equation for the pressure, Equation 11, is differenced as

$$P_i^n + \delta P_i = \left[ (M_{v,i}^n + \delta M_{v,i}) R_v + (M_{a,i}^n + \delta M_{a,i}) R_a \right] \frac{T_i^n}{V_i}. \quad (50)$$

Equations 45 and 46 are then substituted into Equation 50 to eliminate  $\delta M_{v,i}$  and  $\delta M_{a,i}$ . This provides a set of simultaneous linear equations for the incremental changes in pressure in all of the compartments. The solution of this set of equations is currently obtained using a standard linear solver based upon factorization.

After the incremental pressure changes have been determined for all compartments, the suppression pool condensation factors are obtained by simple backward substitution into Equation 47. In turn, the compartment masses are obtained by solving Equations 45 and 46 using the known incremental changes in the compartment pressures. The entrained droplet mass equation, Equation 5, as well as the compartment atmosphere temperature equation, Equation 6, are differenced in a manner similar to Equations 45 and 46 and can be immediately solved using the known pressure increments. It is noted that the present formulation requires that the derivatives of the mass fluxes and the condensation rates with respect to the pressures must be evaluated.

If the mixture temperature calculated with Equation 6 exceeds the saturation temperature at the steam partial pressure and the mixture contains water droplets, then the vaporization/flash rate from the droplets is determined from Equation 8 which is differenced as

$$S_{\text{flash},v,i} = \frac{1}{h_{lv,i}^{n+1}} \left( M_{v,i}^{n+1} C_{v,v} + M_{a,i}^{n+1} C_{v,a} + M_{d,i}^{n+1} C_{p,d} \right) \frac{1}{\delta t} \left( T_i^{n+1} - T_{\text{sat},i}^{n+1} - \frac{dT_{\text{sat},i}}{dP} \frac{\delta t R_v T_i^n S_{\text{flash},v,i}}{V_i} \right). \quad (51)$$

The superscripts,  $n + 1$ , denote partial end of timestep values determined from Equation 6. The last term in Equation 51 accounts for the incremental increase in the saturation pressure from flashing; the flashing rate is therefore given by

$$S_{\text{flash},v,i} = \frac{\frac{1}{h_{lv,i}^{n+1}} \left( M_{v,i}^{n+1} C_{v,v} + M_{a,i}^{n+1} C_{v,a} + M_{d,i}^{n+1} C_{p,d} \right) \frac{1}{\delta t} \left( T_i^{n+1} - T_{\text{sat},i}^{n+1} \right)}{1 + \frac{1}{h_{lv,i}^{n+1}} \left( M_{v,i}^{n+1} C_{v,v} + M_{a,i}^{n+1} C_{v,a} + M_{d,i}^{n+1} C_{p,d} \right) \frac{R_v T_i^n}{V_i}} \quad (52)$$

It is observed that Equation 50 has been formulated using the beginning of timestep temperature. This approach was taken to avoid having to also forward eliminate the entrained droplet mass equation and the temperature equation in terms of the pressure increments. Using the beginning of timestep temperature in this manner has been found not to introduce any significant error into the solution. This behavior reflects the relatively gradual changes in temperature calculated compared with the calculated pressure rises.

The overall flow of the various calculations during an individual timestep are illustrated in Figure 3.

PACER incorporates fairly detailed functional representations of thermodynamic functions for steam/water and steam/water transport properties identical to those employed in the RETRAN-02 code.<sup>7</sup> This provides for a consistent interfacing of PACER with RETRAN calculations of coolant system behavior.

The PACER numerical solution methodology introduces a fair amount of implicitness into the difference equations through consideration of the effects of changes in pressure as represented by the derivatives of the mass fluxes and condensation rates. The pressures inside all compartments are determined simultaneously. This implicit approach is required to permit containment loading calculations to be carried out using large numerical timestep sizes. Most significantly, the timestep need not be chosen restrictively small to preclude the appearance of numerical difficulties such as numerical instabilities when progressively advancing the equations. This feature reduces the overall running time of the code. In practice, the timestep size has been found to be limited only by the accuracy inherent in the first order time differencing of the multicompartment equations.

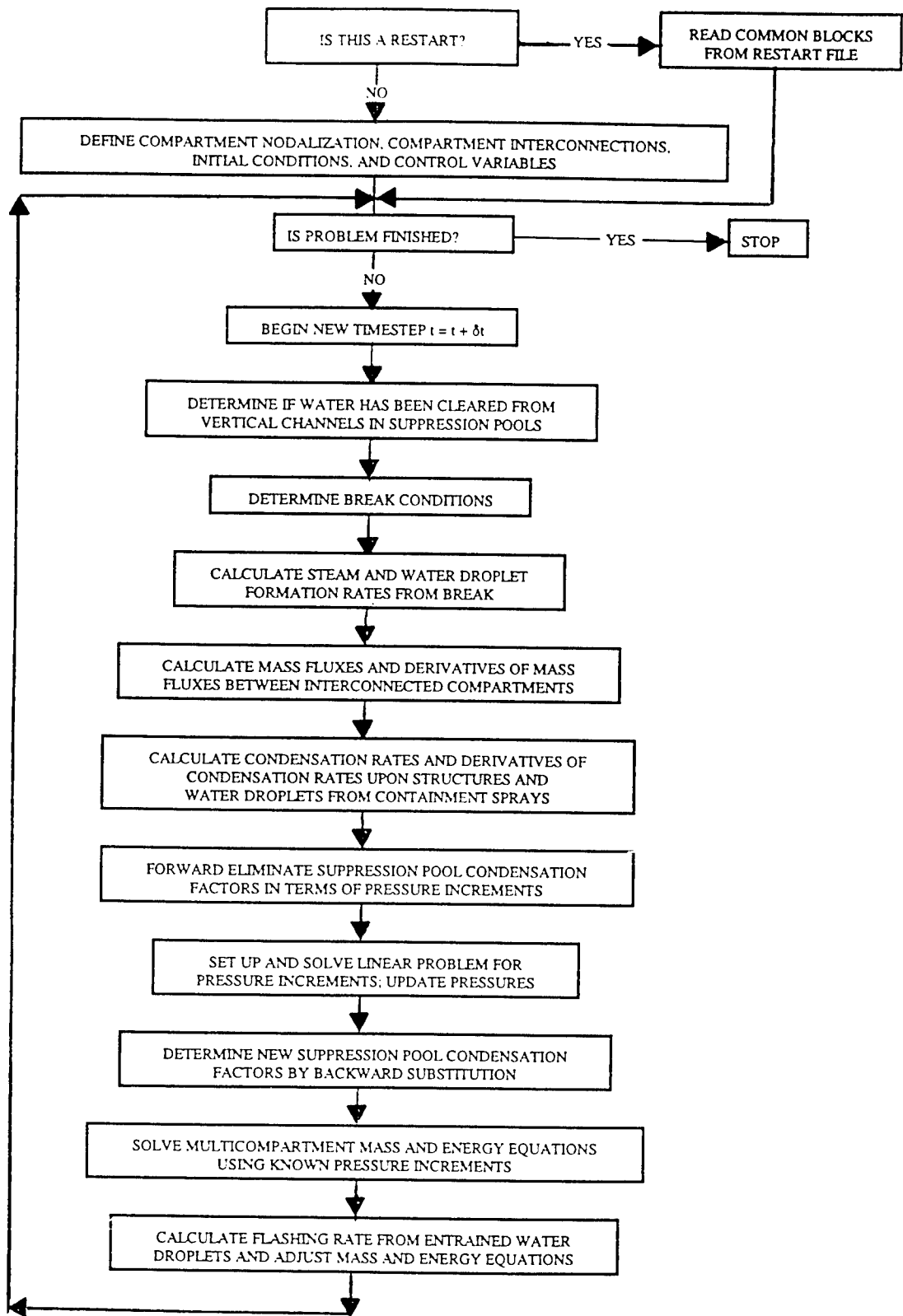


Figure 3. PACER Computational Flow During Problem Setup and Calculation of Transient

## 9.0 SUMMARY

PACER provides a fast running capability to calculate short-term containment/confinement loadings following a postulated failure of the primary or secondary coolant boundary. The code calculates flashing-induced steam formation rates and compartment pressures over a spectrum of break sizes ranging from those representative of small-break LOCAs to large breaks corresponding to a double-ended guillotine pipe rupture. The effects of steam condensation upon structure, intercompartment flow, containment sprays, and water suppression pools are accounted for using best estimate models and correlations often based upon experiment. The multicompartment representation together with the implicit formulation and numerical solution methodology allows for computationally efficient calculations without excessive restrictions upon the timestep size. These features make PACER a useful analytical tool for the analysis of containment/confinement loading phenomena under design basis-type accident conditions as well as for the analysis of short-term loadings in beyond design basis accidents.

## ACKNOWLEDGMENTS

The author is indebted to Dr. B. W. Spencer for his encouragement during the writing of this report and for reviewing the manuscript.

## REFERENCES

1. "Department of Energy's Team's Analyses of Soviet Designed VVER's," DOE/NE-0086, Revision 1, U.S. Department of Energy (September 1989).
2. J. J. Sienicki and W. C. Horak, "Pressure Loadings of Soviet-Designed VVER Reactor Release Mitigation Structures from Large-Break LOCAs," Transactions of the 10th International Conference on Structural Mechanics in Reactor Technology, Anaheim, California, August 14-18, 1989, Vol. J, p. 319.
3. J. M. Kennedy and J. J. Sienicki, "Response of Soviet-Designed VVER-440 Steam Generator Vessel to Pressurization," Transactions of the 10th International Conference on Structural Mechanics in Reactor Technology, Anaheim, California, August 14-18, 1989, Vol. J., p. 325.
4. B. J. Hsieh, R. F. Kulak, P. A. Pfeiffer, J. J. Sienicki, and B. W. Spencer, "Containment Loads and Structural Response for a Large Pipe Break Accident in a VVER-440/213 Nuclear Power Plant," U.S. Department of Energy, Office of Nuclear Energy, Science, and Technology (September 1996).
5. "GOTHIC Containment Analysis Package, Version 3.4e, Volumes 1 through 5," EPRI TR-103053-V1 through TR-10305-V5, Project 3048-01, Final Report (October 1993).
6. K. K. Murata, D. E. Carroll, K. E. Washington, F. Gelbard, G. D. Valdez, D. C. Williams, and K. D. Bergeron, "User's Manual for CONTAIN 1.1 A Computer Code for Severe Nuclear Reactor Containment Analysis," NUREG/CR-5026, SAND 87-2309, Sandia National Laboratories (November 1989).
7. J. H. McFadden et al., "RETAIN-02 - A Program for Transient Thermal-Hydraulic Analysis of Complex Fluid Flow Systems," EPRI NP-1850, Project 889, Final Report, Electric Power Institute (May 1981).
8. H. B. Schwan, "Containment Code Verification by Systematic Evaluation of Experimental Data," Thermal-Hydraulics of Nuclear Reactors. Proceedings of the Second International Topical Meeting on Nuclear Reactor Thermal-Hydraulics, Santa Barbara, California, January 11-14, 1983, Vol. II, p. 1052, American Nuclear Society, LaGrange Park (1983).
9. D. A. Schauer, "Transient Condensation Heat Transfer Coefficient Expressions During and After Blowdown," Fifth International Meeting on Thermal Nuclear Reactor Safety, Karlsruhe, Federal Republic of Germany, September 9-13, 1984, KFK 3880/3, Vol. 3, p. 1850, Kernforschungszentrum, Karlsruhe (December 1984).

M98005659



Report Number (14) ANL-NT--40

\_\_\_\_\_  
\_\_\_\_\_  
\_\_\_\_\_

Publ. Date (11) 1990 06

Sponsor Code (18) DOE/NE, XF

UC Category (19) UC-530, DOE/ER

19980706 100

DOE